

High-Level Parallelism and Nested Features for Dynamic Inference Cost and Top-Down Attention

André Kelm, Niels Hannemann*, Bruno Heberle*, Lucas Schmidt*, Tim Rolff,
Christian Wilms, Ehsan Yaghoubi, Simone Frintrop
Universität Hamburg
Hamburg, Germany

andre.kelm@, Ohannema@informatik., bruno.heberle@, lucas.schmidt-1@studium., tim.rolff@,
christian.wilms@, ehsan.yaghoubi@, simone.frintrop@uni-hamburg.de

Abstract

This paper introduces a novel network topology that seamlessly integrates dynamic inference cost with a top-down attention mechanism, addressing two significant gaps in traditional deep learning models. Drawing inspiration from human perception, we combine sequential processing of generic low-level features with parallelism and nesting of high-level features. This design not only reflects a finding from recent neuroscience research regarding - spatially and contextually distinct neural activations - in human cortex, but also introduces a novel “cutout” technique: the ability to selectively activate only network segments of task-relevant categories to optimize inference cost and eliminate the need for re-training. We believe this paves the way for future network designs that are lightweight and adaptable, making them suitable for a wide range of applications, from compact edge devices to large-scale clouds. Our proposed topology also comes with a built-in top-down attention mechanism, which allows processing to be directly influenced by either enhancing or inhibiting category-specific high-level features, drawing parallels to the selective attention mechanism observed in human cognition. Using targeted external signals, we experimentally enhanced predictions across all tested models. In terms of dynamic inference cost our methodology can achieve an exclusion of up to 73.48% of parameters and 84.41% fewer giga-multiply-accumulate (GMAC) operations, analysis against comparative baselines show an average reduction of 40% in parameters and 8% in GMACs across the cases we evaluated.

1. Introduction

One of the superior capabilities of the human brain is the ability to focus and accelerate processing when high-level knowledge is available. Not only does this save us energy, but it also increases our effectiveness and allows us to act in a very targeted manner. This perceptual ability is still challenging to achieve with current deep learning (DL) methods. If we search for a book on the bookshelf, the salt on the table, or our friend in the crowd, the human visual system is able to focus on target-relevant features and speed up processing considerably: Wolfe’s measurements of human visual perception show that the reaction speed of such a guided visual search is usually significantly higher compared to an unguided search [47]. This aspect is so general that it can also be observed across modalities. A recent neuroscience paper by Marian *et al.* [32], which inspired this work, argues that in the presence of audio signals such as a “meow”, which already allow semantic inferences about a searched object, humans can speed up their visual search and more quickly perceive the object, in this case, the cat. Marian *et al.* assume that there is a contextual connection between modalities and thus, for example, visual category-specific features for objects can be specifically activated. Even with recent DL methods, such behavior cannot be easily reproduced [19]. Widely used attention mechanisms, such as those used in transformer models, tend to be bottom-up, i.e., they focus on the given data [41]. This kind of attention is mainly statistically driven by many images or patches because these are needed for the mechanism to learn which features are more important than others for a particular decision. However, since we want to incorporate cues from the cognitive level (“meow” → “cat”) that include or exclude certain categories in processing, top-down attention is what we need. So the question is: How should we design an artificial neural network that has such focus and accelerated processing capability?

*Niels Hannemann, Bruno Heberle, and Lucas Schmidt contributed equally to this work as part of their bachelor thesis.

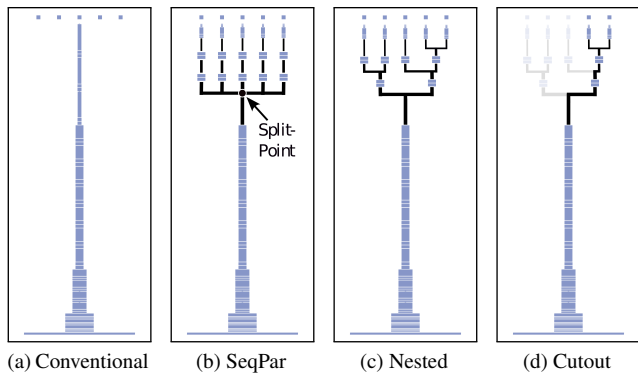


Figure 1. Neural network topologies (blue: tensors, black: connection path). (a) conventional deep network from bottom to top (the dots represent five categories); (b) Our proposed SeqPar structure: each category has its own branch; (c) Our proposed compromise between a and b with a nested structure; (d) Our innovative cutout technique.

We assume that we should be able to exclude irrelevant features from the process to reduce processing time. But DL methods are often described as black boxes [3], so even the visualization of category-specific features is limited [37]. This property makes it challenging to use top-down cues, e.g., target or context information [4], which could be useful to focus on relevant features and speed up processing. Therefore, to access category-specific high-level features that are usually not directly addressable by top-down (context-derived) cues, we restructure, as shown in Fig. 1, the current convention (c.f. 1a) into the proposed **sequential-parallel (SeqPar)** structure (c.f. 1b) and a nested approach (c.f. 1c). Recent neuroscience studies suggest that layer 2 in the primary visual cortex responds in a context-specific way through spatially separated neurons [29, 40, 50], similar to what we intend here: Due to the parallelism of the layers towards the end of the network, features can be separated category-specifically [36]. They can now be amplified by simple scalar weighting, or processed by attention, while low and mid-level features can still be shared by all categories. Intuitively, this makes sense, since they are generic and useful for all categories. But for high-level features it makes less sense because eyes are not useful for cars, for example.

Our contributions are as follows:

- A novel SeqPar structure for category-specific cutouts, as shown in Fig. 1d, consisting of a fixed sequential component and a variable parallel component. These flexible cuts promote a more adaptive model with dynamic inference cost.
- A built-in selective attention mechanism that allows the inference process of an end-to-end learned network to be actively influenced by external signals.

- Nested networks in several variants, allowing the method to be applied to a larger number of categories.

Overall, the SeqPar structure generates category-specific high-level features [51] for another step towards interpretable AI, while providing the ability to bypass unneeded high-level features to reduce parameters, computational cost, and power consumption during inference. This is important for mobile computing, industrial, drone, or robotic applications [6, 7, 43, 45], and because the cost of inference and the cost of training for AI models used in industry is up to 9:1 [14].

2. Related Work

2.1. Image Classification and Dynamic Inference

In the field of computer vision (CV), image classification is a key task, with ImageNet [13] validation traditionally serving as a benchmark [52]. Powerful models developed for this task are then often applied to a variety of other areas, from semantic segmentation to object detection and video recognition [30]. This field is evolving rapidly, so methods such as transformers [53], large language models [5], knowledge distillation [8], wild and large datasets [31], unsupervised learning [9], and matching loss functions [44], etc. are constantly advancing the state-of-the-art. Larger and deeper models often offer an accuracy advantage [15], but this leads to increasing training and inference costs [14]. Notably, the industry tends to prioritize reducing inference costs over training costs by a factor of 9 [14], so a great variety of work has been done to dynamize inference costs [20]. Dynamic routing, dynamic blocks and channels trained end-to-end are promising methods [42]. However, the possibility of dynamizing the inference process by activating only target-relevant features depending on the task and context is not so often taken into account. Such an implemented adaptation could save parameters, energy, and processing time. This is where our method comes in, so that high-level features can be generated category-specifically by parallelization and excluded when not needed.

2.2. Bottom-up vs. Top-Down Attention

Selective attention is a mechanism of human perception that enables us to focus on regions of potential interest [11, 28]. These can be objects, colors, locations, sounds, or other patterns. It helps us to deal with the complexity of the world and to quickly find objects of interest. Attention is driven by two types of cues: bottom-up and top-down cues [39]. Bottom-up cues are salient patterns that automatically attract attention, such as a red flower on green grass. Top-down attention, on the other hand, focuses on regions which are behaviorally relevant and is driven by pre-knowledge, goals, or expectations. Searching for our key,

or the well-known cocktail-party effect [2] are examples of top-down attention.

Attention mechanisms have become very popular in DL [12]. However, most of them cannot focus in a top-down manner like biological systems. They usually base their processing on the input data and do not consider pre-knowledge about the target or the scene. Early works before the DL era have amplified target-relevant features by excitation and inhibition of pre-computed features to realize top-down attention [18, 33]. In deep networks, top-down attention is usually understood as a tracing of activations backwards through the network from class nodes to the feature maps, as in GradCAM [37], and is often used to localize class-specific features in feature maps. However, this requires one forward-pass of the input image through the network, before the backward tracing can be performed, and does not enable a quicker processing through the usage of pre-knowledge as in human perception.

2.3. Parallelism and Tree Networks

Parallelism, as we introduce it in this work, is rarely used and, as far as we know, unique to this extent and in the context of dynamic inference or selective attention. At first sight, it’s reminiscent of ensemble learning, where multiple neural networks are trained side by side, e.g., to solve a task very precisely [1, 27], but it differs in the following point: Ensembles often use multiple models, sometimes with specialized input, to train experts, whereas we train a single model with multiple branches and input from all categories, characterized by a SeqPar structure. Thus, low-level and mid-level features can still be shared by all categories, while high-level features are separated in a category-specific way.

A work more related to ours than previously listed ones is the tree-like branching (TLB) network from Xue *et al.* [51] with a category-specific branching. They propose a tree structure based on the similarities of the categories and show improvements for image classification. They do not draw parallels to brain inspiration or a relation to selective attention and therefore do not perform experiments in this direction, and although they show improved inference costs, they do so for the model as a whole and do not use the novelty of inference cost dynamization by cutouts introduced here. The architecture, nesting, and approach to nesting are also different.

3. Proposed Method

Current DL methods, unlike biological systems, cannot easily accelerate or focus their processing in scenarios where high-level knowledge from other modalities or insights are available [32]. They typically lack mechanisms for dynamically adjusting inference costs [49] or incorporating top-down attention [4], which would intuitively require focusing on specific features. Due to their “black-

| lay./mod. | PHL _{small} | PHL _{big} | PHL _{lateSP} | ResNet50 |
|-----------|---|---|--|----------|
| input | 224 × 224 × 3 | | | |
| conv 1 | 7 × 7 × 3 × 64, stride 2 | | | |
| pool 1 | 3 × 3, max | | | |
| output | 56 × 56 | | | |
| conv 2a | 1 × 1 × 64 | | | |
| conv 2b | 3 × 3 × 64 | | | |
| conv 2c | 1 × 1 × 64 × 64/256 | | | |
| reps | 3 | | | |
| output | 28 × 28 | | | |
| conv 3a | 1 × 1 × 256 × 128 | | | |
| conv 3b | 3 × 3 × 128 × 128 | | | |
| conv 3c | 1 × 1 × 128 × 128/512 | | | |
| reps | 4 | | | |
| output | 14 × 14 | | | |
| conv 4a | 1×1×512×128 | 1×1×512×256 | | |
| conv 4b | 3×3×128×128 | 3×3×256×256 | | |
| conv 4c | 1×1×128×512 | 1×1×256×256/1024 | | |
| reps | 1 | | | 6 |
| par | k | | | 1 |
| output | 7×7 | | | |
| conv 5a | 1×1×512×64 | 1×1×1024×128 | 1×1×1024×512 | |
| conv 5b | 3×3×64×64 | 3×3×128×128 | 3×3×512×512 | |
| conv 5c | 1×1×64×256 | 1×1×128×512 | 1×1×256×512/2048 | |
| reps | 1 | | | 3 |
| Par | k | k | 1 | |
| output | 3 × 3 | | | |
| conv 6a | 1×1×256×32 | 1×1×512×64 | | |
| conv 6b | 3×3×32×32 | 3×3×64×64 | | |
| conv 6c | 1×1×32×128 | 1×1×64×256 | | |
| reps | 1 | | | |
| par | k | k | 1 | |
| output | 1 × 1 | | 3 × 3 | |
| conv 7a | | | 1×1×256×32 | |
| conv 7b | | | 3×3×32×32 | |
| conv 7c | | | 1×1×32×128 | |
| reps | | | 1 | |
| par | | | k | |
| output | 1 × 1 | | 3 × 3 | |
| pool&flat | 3 × 3 average pooling + flatten layer | | | |
| FC | 128 | 256 | 128 | 2048 |
| output | 1 × 1 × 1 × k | | | |

Table 1. Detailed model architectures. Left: three variants of our PHL method; right: a ResNet50 of conventional type. The red boxes indicate the location of the split-point which introduces the main change of the network topology: PHLs get as many parallel branches as the categories k to be recognized; ResNets have only one. On the other hand, PHL has fewer Seq repetitions (abbreviated as reps) of conv blocks - resulting in a shallower net. The green box is the insertion point for a second hierarchy level for NHL_{wordnet} and the blue one marks a third hierarchy for NHL_{gpt}.

box” nature [3], most models do not even reveal where category-specific features are located in the deep network. To overcome these challenges, we rethink the conventional, mostly sequential network topology and propose a SeqPar system that provides distinct and assignable layers for different categories. Recent neuroscientific studies support our approach and show that the human brain also has context-specific areas [29, 50].

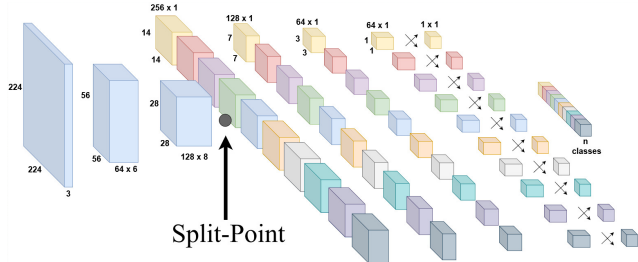


Figure 2. Our PHL architecture starts sequentially, but becomes parallel after a split-point to generate category-specific features that are spatially separated from each other. The different colors represent the categories and their branches. The resolution and the dimension of the feature channel, multiplied by the number of layers have exemplary values for a better understanding.

3.1. High-Level Feature Parallelization

We are exploring a new network topology, whose principle can be applied to modern models. Therefore, we have based our model on a widely known standard, the ResNet50. Fig. 2 shows our proposed **Parallelize** features at a **High-Level** network (**PHL**). We define the PHL by several blocks containing several layers. It can be divided into two parts: the first layers, which are classically sequential, and the deeper layers, which have the novel parallel information flow, all including ResNet skip connections. In Tab. 1 we have listed three variants. They differ by having fewer (small) or more (big) channels per parallel branch or by a later split-point (lateSP). The hypothesis behind splitting the architecture into multiple branches while simultaneously processing the initial input through a sequential network is that lower-level features are generic and useful for almost any category, while higher-level features are more specific, e.g., eye features are not required for a car and should therefore be treated in parallel. We define this connection as the **split-point** that connects the two parts of the network. Intuitively, a split-point could benefit from a larger number of parameters as it has to handle $1 : k$ connections, so we use a bottleneck structure [21].

Split-Point: Formally, we define the first part of our architecture to consist of shared network layers up to the split-point through the function: $\phi(x, \theta_0)$, taking the input image x and network parameters θ_0 as input. As we provide a branch for each of the target categories k , we define the number of final branches to be the same as our k target categories. Hence, we use k branch networks that we define through $\psi(\bar{x}, \theta_i)$ with $1 \leq i \leq k$, which take the output features of ϕ as input for \bar{x} . As all branch networks have the same design, we only exchange the network parameters θ_i for the classification of the i^{th} class. Using the above definitions allows us to define the output of the i^{th} branch

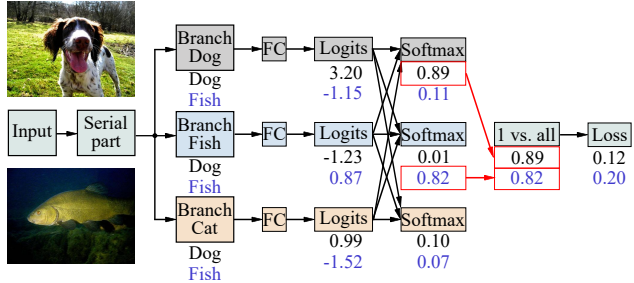


Figure 3. Three-branched PHL network for dog, fish and cat categories with some example values (black: input dog, blue: input fish). The red boxes indicate the selection for 1 vs. all. Images from Imagenette [22].

network, which is responsible for class i , as:

$$f_i(x) = \psi(\phi(x, \theta_0), \theta_i) = y_i. \quad (1)$$

Cross-Entropy Loss: For training of the network, we retain all initial target categories and estimate the class probability over all categories for the likelihood of an input x belonging to a class and utilized a cross-entropy as our loss function. Note also that this is the special case of Eq. 3 where we utilized all categories instead of a subset. The result of the likelihood estimation is included in a 1 vs. all classification and the cross entropy loss, see details in Fig. 3. Optimizing the loss through backpropagation results in a high-value output for an image that belongs to the branch and a low-value output otherwise. Due to the softmax function, all paths are learned at once. Fig. 3 illustrates this central point of our approach.

3.2. Nested Topology

By pursuing the idea of category-dependent feature similarity and feature sharing at different hierarchical levels between image categories, we assume that a more optimal network topology can be constructed by nesting branches depending on the categories and their superclasses. We hypothesize that there are higher-level features that should be shared, such as wheels for buses and cars, and propose the **Nest** features at a **High-Level** (**NHL**) network. Fig. 1c shows a schematic of such an architecture. To get an additional level of hierarchy, we use the superclasses provided by imagenet-superclass [35] and Wordnet [16] for ImageNet categories [13]. Using these, we define this extended architecture by introducing another split-point, indicated by the green box for PHL-small in Tab. 1. Here, multiple branches i share the features of a superclass j through an additional sub-network $\pi(\hat{x}, \hat{\theta}_j)$ with network parameters $\hat{\theta}$ and again taking the output of ϕ as input for \hat{x} and passing its output to \bar{x} of ψ . Hence, a total number of superclasses s results in an equal number of branches $1 \leq j \leq s$ in the

lower hierarchical layer. Note that this does not change the total number of terminal branches k in the upper hierarchical layer, since they are still equal to the number of categories in the dataset. This allows us to redefine the output of the hierarchical branching network:

$$\hat{f}_i(x) = \psi(\pi(\phi(x, \theta_0), \hat{\theta}_j), \theta_i) = y_i. \quad (2)$$

To train the network, we use the aforementioned cross-entropy loss and our redefined softmax. In developing more nesting variants with three or four split-points in a fast and easy way, we consider several suggestions from OpenAI’s ChatGPT4 [34].

NHL_{gpt}: In the case of just two split-points, there is a high number of possible branch nestings, exceeding $B_{100} \approx 10^{115}$ for 100 and $B_{1000} \approx 10^{1927}$ for 1000 categories, with B_n being the Bell function [38]. Yet, for a network with just one split-point this number is equal to one, as it does not allow rearranging as the number of categories is fixed. Hence, for a three hierarchy levels deep network N3HL_{gpt}, we employed a hybrid semi-automatic approach using ChatGPT. Here, we leveraged ChatGPT whenever the classification was ambiguous.

3.3. Cutouts

Conventional architectures usually do not have the ability to omit category-specific high-level features that are not needed. Often it is not even clear which parameter contributes to which category. However, if only a subset of categories is needed for a specific task - whether by changed conditions or due to prior semantic knowledge - an option to exclude category-specific features would be advantageous. Through the above made definition of a split-point, we can define cutouts that allow the network to adapt to simpler tasks in the case that prior knowledge is available. This enables the formation of selected category-specific paths that are shorter and faster than if a standard neural network has to be used (c.f. 4). Here, we extract $n \leq k$ selected paths using a-priori knowledge of potential n new target categories $C = \{i_0, \dots, i_n \mid 1 \leq i_j \leq k\}$, while simultaneously keeping the branch fully functional. This allows us to define the probability of a sample belonging to that category $i \in C$ through:

$$p_i(x) = \frac{e^{-f_i(x)}}{\sum_{j \in C} e^{-f_j(x)}}. \quad (3)$$

The ability to adapt to the lower complexity of a task with less computational effort, but also to increase it when needed, is reminiscent of efficient and effective biological systems and their ability to focus.

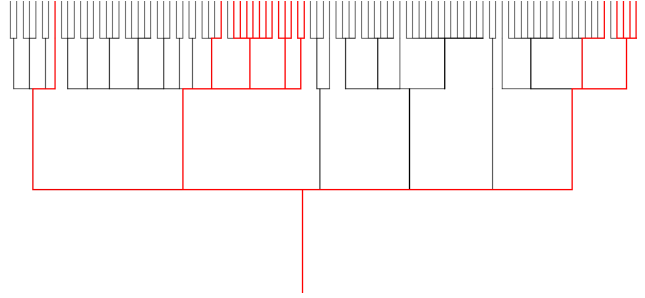


Figure 4. Cutout from a N3HL network with 100 categories. The red pathways highlight the activated paths for the selected 20 categories from ImageNet100 [22], demonstrating the “cutout” technique (processing from bottom to top).

4. Experiments

We evaluate five of our proposed topology variants PHL (see Sec. 3.1), N2HL, N3HL and N4HL (see Sec. 3.2) by implementing them using ResNet50 and the N3HL152 by using ResNet152 and compare them with their conventional counterpart. We include ResNet18 and -200 to measure some lower and upper performance limits. Our unique top-down attention mechanism (see Sec. 4.4) is tested for PHL and NHL, highlighted in light gray in the respective tables and underlined with TD attention. It is worth mentioning, that these are not separate models, as they are subject to amplification of targeted feature maps by external signals, this technique is applicable to all PHL or NHL networks.

4.1. Training and Datasets

We have implemented all our models in the Timm library [46] and used Rand Augment [10]. We used three different levels of classification complexity and training setups for studying PHL and NHL:

- 10 categories with 1000 epochs, batch size 32
- 100 categories with 300 epochs, batch size 56, maxed out 24, 564 MebiBytes (MiB), mixed precision training
- 1000 categories with 300 epochs and batch size 24, and another run with batch size 46, maxed out 24, 564 and 49, 140 MiB, both trained through mixed precision training

As datasets, we chose subsets of ImageNet [13]. Imagenette and Imagewoof [22] both contain 10 categories, with the interesting property that Imagenette contains categories, which differ considerably, while Imagewoofs categories are quite similar (breeds of dogs). Testing these two datasets helps to understand how the parallel branches handle similar and non-similar categories. ImageNet100 [13, 23] has some similar and some differing categories, but shows how the

model handles an upscaling by a factor of 10. The datasets used here have similar category and image numbers, and therefore a similar significance to Cifar10 and -100. These are not used because their lower image resolution would introduce an unwanted new factor into the evaluation [24,25]. ImageNet mini [17] is a subset of ImageNet1k and has only a few images per category, about 20-50, but offers a high classification complexity with 1000 categories. We evaluate the top-1 accuracy and omit the top-5, as this does not carry much meaning for the datasets with few categories.

4.2. Dynamic Inference Cost

The cutouts presented in Sec. 3.1 are a unique property of PHL or NHL, where parameters are reduced by focusing only on the remaining and relevant categories, adapting to a changing task without requiring re-training. For the evaluation in Tab. 2, we have divided the datasets into two subsets: lower label categories (e.g., category-ID: 1-5) and upper label categories (e.g., category-ID: 6-10). To start somewhere, we divide the 10 categories 50:50 and the 100 categories 80:20. For the baseline, we have ResNets that are trained like the cutouts on the full dataset and validated only on the subset, and ResNets that are completely new trained only on the subset. For Imagenette upper and lower 5 the cutouts have a better top-1 acc. than newly trained ResNets. Slightly better are the ResNets, also trained on 10 categories, but the cutouts are able to reduce the parameters by approximately 28%. To determine the computational complexity, we count giga-multiply-accumulate operations (GMACs) and find that we can save about 8% while maintaining very high performance. In Imagewoof, the cutouts have a top-1 acc. with high values for the upper and a little worse for the lower 5, but when considering both accuracies its better and again with a reduction of parameters and GMACs. For ImageNet100 we show a cutout of 20 categories. It's the same cutout as used in the visualization in Fig. 4. The cutout has the best result only slightly increasing the GMACs but with a reduction of about 10 million parameters. The last cutout at the bottom shows an evaluation from ImageNet1k.

It is a good result for our method in terms of accuracy, due to the same and a little better acc. than the baseline, but with fewer GMACs, fewer parameters and less depth. More importantly, it builds on the example of cross-modal interaction presented in the introduction of our paper by Marian et al. [32], our approach can use already interpreted semantic cues such as the sound “meow” to focus visually. This allows the model to efficiently narrow down from 1000 learned categories of ImageNet to the 5 relevant ones, representing domestic cats. This demonstrates the practical application of our method with a high dynamic range of inference costs.

| dataset | Imagenette | | |
|-------------------------------|-------------------|-------------------|---------------------------|
| model | ResNet50 | | PHL _{lateSP} |
| GMACs | 4.13 | | 3.99 |
| GMACs cutout | NA | | 3.66 |
| GMACs. reduction | 0 % | | -8.40 % |
| parameter | 23, 518, 277 | 23, 528, 522 | 19,986,506 |
| param. cutout | NA | | 14,264,901 |
| param. reduction | 0 % | | -28.63 % |
| train categories | upper 5 | all 10 | all 10 |
| val categories | upper 5 | upper 5 | upper 5 |
| top-1 accuracy | 97.16 | 97.83 | 97.62 |
| train categories | lower 5 | all 10 | all 10 |
| val categories | lower 5 | lower 5 | lower 5 |
| top-1 accuracy | 96.79 | 98.04 | 98.04 |
| dataset | Imagewoof | | |
| model | ResNet50 | | N3HL _{gpt} |
| GMACs | 4.13 | | 3.91 |
| GMACs cutout | NA | | 3.73 |
| GMACs reduction | 0 % | | -4.90 % |
| parameter | 23, 518, 277 | 23, 528, 522 | 11,929,930 |
| param. cutout | NA | | 10,781,253 |
| param. reduction | 0 % | | -9.63 % |
| train categories | upper 5 | all 10 | all 10 |
| val categories | upper 5 | upper 5 | upper 5 |
| top-1 accuracy | 91.18 | 91.88 | 92.69 |
| train categories | lower 5 | all 10 | all 10 |
| val categories | lower 5 | lower 5 | lower 5 |
| top-1 accuracy | 96.23 | 94.30 | 95.89 |
| dataset | ImageNet100 | | |
| model | ResNet50 | | N3HL _{gpt} |
| GMACs | 4.13 | | 5.86 |
| GMACs cutout | NA | | 4.22 |
| GMACs. reduction | 0 % | | -27.99 % |
| parameter | 23,549,012 | 23,712,932 | 24, 950, 436 |
| param. cutout | NA | | 13,840,469 |
| param. reduction | 0 % | | -44.53 % |
| train categories | lower 20 | all 100 | all 100 |
| val categories | lower 20 | lower 20 | lower 20 |
| top-1 accuracy | 88.50 | 90.60 | 93.40 |
| top-1 _{TD attention} | NA | NA | 94.20 |
| dataset | ImageNet1k | | |
| model | ConvNeXtV2 | | ConvNeXtV2 _{NHL} |
| GMACs | 4.56 | | 14.55 |
| GMACs cutout | NA | | 3.87 |
| GMACs. reduction | 0 % | | -73.40 % |
| parameter | 27,801,029 | 28,566,184 | 119, 879, 336 |
| param. cutout | NA | | 13,488,133 |
| param. reduction | 0 % | | -88.74 % |
| train categories | meow 5 | all 1000 | all 1000 |
| val categories | meow 5 | meow 5 | meow 5 |
| top-1 accuracy | 80.00 | 79.60 | 80.00 |

Table 2. Dynamic inference costs of six cutouts compared to ResNet50. For Imagenette and Imagewoof, the analysis is divided into two subsets: upper (first x categories) and lower (remaining y categories). ImageNet100 dataset is evaluated with a 20-category cutout, while ImageNet mini focuses on a cutout specific to cat.

4.3. Image Classification

For this task there are three baselines, so for better comprehensibility the Tab. 3 is also split into three sections:

| Dataset | Imagenette | | Imagewoof | ImageNet100 | | ImageNet mini | ImageNet1k |
|-------------------------------|---------------|----------------------|--------------|-----------------------|--------------|------------------------|--------------|
| | no. parameter | top-1 acc. | top-1 acc. | no. parameter | top-1 acc. | no. parameter | top-1 acc. |
| PHL _{small} (base 1) | 9,611,338 | 95.71 | 89.97 | 83,109,028 | 82.52 | 818,213,928 | 21.10 |
| PHL _{TD attention} | 9,611,338 | 96.38 | 90.54 | 83,109,028 | 82.56 | 818,213,928 | 21.34 |
| ResNet50 (base 2) | 23,528,522 | 96.15 | 90.30 | 23,712,932 | 85.34 | 25,557,032 | 33.38 |
| ResNet18 | 11,181,642 | 95.52 | 89.97 | 11,227,812 | 81.76 | 11,689,512 | 28.52 |
| N2HL _{wordnet} | - | NA | NA | 65,725,604 | 84.02 | 577,977,384 | 19.98 |
| N3HL _{gpt} | 11,929,930 | 96.18 | 91.65 | 24,950,436 | 85.68 | 113,547,048 | 31.78 |
| ResNet152 (base 3) | 58,164,298 | 96.33 | 90.89 | 58,348,708 | 86.24 | 60,192,808 | 31.12 |
| ResNet200 | - | - | - | 62,829,732 | 87.02 | 64,673,832 | 31.97 |
| N3HL152 _{gpt} | - | - | - | 59,586,212 | 87.08 | 148,182,824 | - |
| | | 10 categories | | 100 categories | | 1000 categories | |

Table 3. The image classification results are divided into three table sections, each compared with its own respective baseline for fair evaluation. Top (base 1): External signals on PHL_{small} simulate top-down attention. Middle (base 2): NHL_{gpt} vs. ResNet50. Bottom (base 3): NHL152_{gpt} vs. ResNet152. Symbol - is used to exclude irrelevant data.

Base 1: For 10 categories the PHL nets have a top-1 acc. below the ResNets. This can be seen in the top section. When scaling the PHL to 100 or 1000 categories, the performance drops even more.

Base 2: The later split-point and nesting show significant progress and lift our approaches N3HL und N4HL_{gpt} above the ResNet50 for 10 and 100 categories, only for 1000 the methodology remains below. However, this may be due to the fact that Imagenet mini has so few training and validation images, which probably has a negative effect on our approach due to the higher number of parameters for 1000 categories. N2HL_{wordnet} cannot keep up, because the split-point was set too early or the nesting is not so advantageous.

Base 3: Our N3HL153_{gpt} method can also outperform deeper networks such as the ResNet152 and the even deeper ResNet200 for Imagenet100. To show that the N3HL152_{gpt} remains competitive even with 1000 categories, we trained the methods on ImageNet1k and ours is ahead of the similarly deep ResNet152.

4.4. Built-in Top-Down Attention

Consider a task where objects shall be classified in images and other modalities such as audio or descriptions are already available and provide prior semantic knowledge. This leads to contextual cues that can positively influence the classification, e.g. a “meow” should strengthen the classification of the object “cat” as in human perception [47].

We argue that the proposed PHL has a built-in selective attention mechanism because we know where to access the category-specific high-level features, since individual feature maps can be associated with a branch, its parameters, and a category. Fig. 5 visualizes the feature maps of two parallel branches and shows category-specific differences. In an initial test, we assume that meaningful semantic knowledge already exists for each validation image, so that amplification should be done for each image category. This is done by simply multiplying the feature maps in the corresponding path in conv block 5 of PHL_{small} (see Tab. 1) by a scalar. Here we use values of 1.8 (Ima-

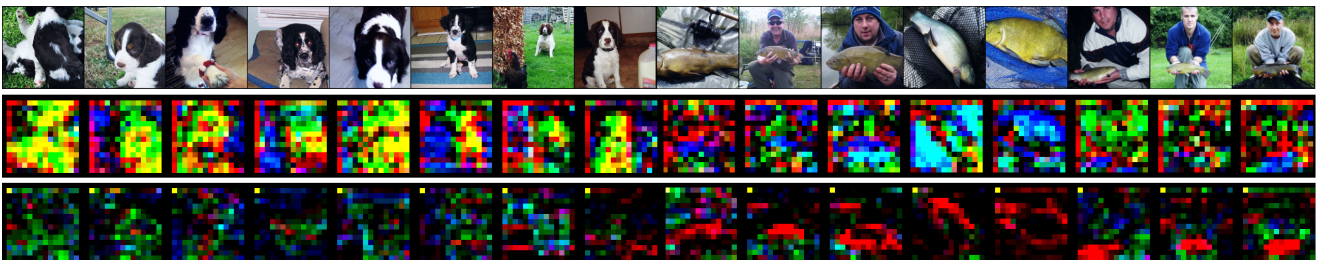


Figure 5. Category-specific features and original images from Imagenette [22]. The top row displays the images at a reduced resolution. The second and third rows show $14 \times 14 \times 3$ RGB-colored, category-specific high-level features extracted using PHL_{big} - conv 4. Specifically, the features in the second row are from the “dog” branch, while the features in the third row from the “fish” branch. The selected feature maps from the dog branch are salient for the dog object and less salient for the fish object. The opposite is observed for the fish branch.

This advancement holds substantial promise for mobile computing, industrial, drone, robotic, and edge device applications, where computational resources are often limited. Future research could further refine these topologies, potentially leading to breakthroughs in artificial intelligence that more closely resemble human cognitive processes.

References

- [1] Sanghyeon An, Min Jun Lee, Sanglee Park, He Sarina Yang, and Jungmin So. An ensemble of simple convolutional neural network models for mnist digit recognition. *ArXiv*, abs/2008.10400, 2020. 3
- [2] Barry Arons. A review of the cocktail party effect. *Journal of the American Voice I/O Society*, 12(7):35–50, 1992. 3
- [3] Caglar Aytekin. Neural networks are decision trees. *ArXiv*, abs/2210.05189, 2022. 2, 3
- [4] Soubarna Banik, Mikko Lauri, Alois Knoll, and Simone Frintrop. Object localization with attribute preference based on top-down attention. In Markus Vincze, Timothy Patten, Henrik I. Christensen, Lazaros Nalpantidis, and Ming Liu, editors, *Computer Vision Systems*, pages 28–40, Cham, 2021. Springer International Publishing. 2, 3
- [5] Tom Brown, Benjamin Mann, Nick Ryder, Melanie Subbiah, Jared D Kaplan, Prafulla Dhariwal, Arvind Neelakantan, Pranav Shyam, Girish Sastry, Amanda Askell, Sandhini Agarwal, Ariel Herbert-Voss, Gretchen Krueger, Tom Henighan, Rewon Child, Aditya Ramesh, Daniel Ziegler, Jeffrey Wu, Clemens Winter, Chris Hesse, Mark Chen, Eric Sigler, Matusz Litwin, Scott Gray, Benjamin Chess, Jack Clark, Christopher Berner, Sam McCandlish, Alec Radford, Ilya Sutskever, and Dario Amodei. Language models are few-shot learners. In H. Larochelle, M. Ranzato, R. Hadsell, M.F. Balcan, and H. Lin, editors, *Advances in Neural Information Processing Systems*, volume 33, pages 1877–1901. Curran Associates, Inc., 2020. 2
- [6] Widodo Budiharto, Alexander A S Gunawan, Jarot S. Suroso, Andry Chowanda, Aurello Patrik, and Gaudi Utama. Fast object detection for quadcopter drone using deep learning. In *2018 3rd International Conference on Computer and Communication Systems (ICCCS)*, pages 192–195, 2018. 2
- [7] Han Cai, Ji Lin, Yujun Lin, Zhijian Liu, Haotian Tang, Hanrui Wang, Ligeng Zhu, and Song Han. Enable deep learning on mobile devices: Methods, systems, and applications. *ACM Trans. Des. Autom. Electron. Syst.*, 27(3), mar 2022. 2
- [8] Mathilde Caron, Hugo Touvron, Ishan Misra, Hervé Jegou, Julien Mairal, Piotr Bojanowski, and Armand Joulin. Emerging properties in self-supervised vision transformers. In *2021 IEEE/CVF International Conference on Computer Vision (ICCV)*, pages 9630–9640, 2021. 2
- [9] Ting Chen, Simon Kornblith, Mohammad Norouzi, and Geoffrey Hinton. A simple framework for contrastive learning of visual representations. In *Proceedings of the 37th International Conference on Machine Learning*, ICLR’20. JMLR.org, 2020. 2
- [10] Ekin D. Cubuk, Barret Zoph, Jonathon Shlens, and Quoc V. Le. Randaugment: Practical automated data augmentation with a reduced search space. In *2020 IEEE/CVF Conference on Computer Vision and Pattern Recognition Workshops (CVPRW)*, pages 3008–3017, 2020. 5
- [11] Elizabeth T Davis and John Palmer. Visual search and attention: an overview. *Spatial Vision*, 2004. 2
- [12] Alana de Santana Correia and E. Colombini. Attention, please! a survey of neural attention models in deep learning. *Artificial Intelligence Review*, 55:6037 – 6124, 2022. 3
- [13] Jia Deng, Wei Dong, Richard Socher, Li-Jia Li, Kai Li, and Li Fei-Fei. Imagenet: A large-scale hierarchical image database. In *2009 IEEE conference on computer vision and pattern recognition*, pages 248–255. Ieee, 2009. 2, 4, 5
- [14] Radosvet Desislavov, Fernando Martínez-Plumed, and José Hernández-Orallo. Trends in ai inference energy consumption: Beyond the performance-vs-parameter laws of deep learning. *Sustainable Computing: Informatics and Systems*, 38:100857, 2023. 2
- [15] Y. Fang, W. Wang, B. Xie, Q. Sun, L. Wu, X. Wang, T. Huang, X. Wang, and Y. Cao. Eva: Exploring the limits of masked visual representation learning at scale. In *2023 IEEE/CVF Conference on Computer Vision and Pattern Recognition (CVPR)*, pages 19358–19369, Los Alamitos, CA, USA, jun 2023. IEEE Computer Society. 2
- [16] Christiane Fellbaum. *WordNet: An Electronic Lexical Database*. Bradford Books, 1998. 4
- [17] Ilya Figotin. Imagenet 1000 (mini). <https://www.kaggle.com/datasets/ifigotin/imagenetmini-1000>, Mar 2020. 6
- [18] Simone Frintrop, Gerriet Backer, and Erich Rome. Goal-directed search with a top-down modulated computational attention system. In *Pattern Recognition: 27th DAGM Symposium, Vienna, Austria, August 31-September 2, 2005. Proceedings 27*, pages 117–124. Springer, 2005. 3
- [19] Di Fu, Cornelius Weber, Guochun Yang, Matthias Kerzel, Weizhi Nan, Pablo Barros, Haiyan Wu, Xun Liu, and Stefan Wermter. What can computational models learn from human selective attention? a review from an audiovisual unimodal and crossmodal perspective. *Frontiers in Integrative Neuroscience*, 14, 2020. 1
- [20] Yizeng Han, Gao Huang, Shiji Song, Le Yang, Honghui Wang, and Yulin Wang. Dynamic neural networks: A survey. *IEEE Transactions on Pattern Analysis and Machine Intelligence*, 44(11):7436–7456, 2022. 2
- [21] K. He, X. Zhang, S. Ren, and J. Sun. Deep residual learning for image recognition. In *2016 IEEE Conference on Computer Vision and Pattern Recognition (CVPR)*, pages 770–778, June 2016. 4
- [22] Jeremy Howard. Imagewang. <https://github.com/fastai/imagenette/>. 4, 5, 7
- [23] kaggle. Imagenet100. <https://www.kaggle.com/datasets/ambityga/imagenet100>, 2020. Accessed: 2023-11-17. 5
- [24] Alex Krizhevsky, Vinod Nair, and Geoffrey Hinton. Cifar-10 (canadian institute for advanced research). 6
- [25] Alex Krizhevsky, Vinod Nair, and Geoffrey Hinton. Cifar-100 (canadian institute for advanced research). 6

- [26] Ting-Yu Kuo, Yuanda Liao, Kai Li, Bo Hong, and Xiaolin Hu. Inferring mechanisms of auditory attentional modulation with deep neural networks. *Neural Computation*, 34(11):2273–2293, 2022. 8
- [27] Retno Larasati and Hak KeungLam. Handwritten digits recognition using ensemble neural networks and ensemble decision tree. In *2017 International Conference on Smart Cities, Automation & Intelligent Computing Systems (ICONSONICS)*, pages 99–104, 2017. 3
- [28] Tidhar Lev-Ari, Hadar Beeri, and Yoram Gutfreund. The ecological view of selective attention. *Frontiers in Integrative Neuroscience*, 16, 2022. 2
- [29] Kai-Yuan Liu, Xing-Yu Li, Yu-Rui Lai, Hang Su, Jia-Chen Wang, Chun-Xu Guo, Hong Xie, Ji-Song Guan, and Yi Zhou. Denoised internal models: A brain-inspired autoencoder against adversarial attacks. *Machine Intelligence Research*, 19(5):456–471, Oct 2022. 2, 3
- [30] Z. Liu, J. Ning, Y. Cao, Y. Wei, Z. Zhang, S. Lin, and H. Hu. Video swin transformer. In *2022 IEEE/CVF Conference on Computer Vision and Pattern Recognition (CVPR)*, pages 3192–3201, Los Alamitos, CA, USA, jun 2022. IEEE Computer Society. 2
- [31] Dhruv Mahajan, Ross Girshick, Vignesh Ramanathan, Kaiming He, Manohar Paluri, Yixuan Li, Ashwin Bharambe, and Laurens van der Maaten. Exploring the limits of weakly supervised pretraining. In *Computer Vision – ECCV 2018: 15th European Conference, Munich, Germany, September 8-14, 2018, Proceedings, Part II*, page 185–201, Berlin, Heidelberg, 2018. Springer-Verlag. 2
- [32] Viorica Marian, Sayuri Hayakawa, and Scott R. Schroeder. Cross-modal interaction between auditory and visual input impacts memory retrieval. *Frontiers in Neuroscience*, 15, 2021. 1, 3, 6
- [33] Vidhya Navalpakkam and Laurent Itti. Modeling the influence of task on attention. *Vision research*, 45(2):205–231, 2005. 3
- [34] OpenAI. Chatgpt. <https://openai.com/>, 2023. 5
- [35] S-Kumano. S-kumano/imagenet-superclass: The example of correspondence between fine classes and superclass (coarse class) in imagenet. <https://github.com/s-kumano/imagenet-superclass>. 4
- [36] Ali Sekmen, Mustafa Parlaktuna, Ayad Abdul-Malek, Erdem Erdemir, and Ahmet Buğra Koku. Robust feature space separation for deep convolutional neural network training. *Discover Artificial Intelligence*, 1(12):1–11, 2021. 2
- [37] Ramprasaath R Selvaraju, Michael Cogswell, Abhishek Das, Ramakrishna Vedantam, Devi Parikh, and Dhruv Batra. Grad-cam: Visual explanations from deep networks via gradient-based localization. In *Proceedings of the IEEE international conference on computer vision*, pages 618–626, 2017. 2, 3
- [38] Stephen M. Tanny. On some numbers related to the bell numbers. *Canadian Mathematical Bulletin*, 17(5):733–738, 1975. 5
- [39] Jan Theeuwes. Top-down and bottom-up control of visual selection. *Acta psychologica*, 135(2):77–99, 2010. 2
- [40] Susumu Tonegawa, Xu Liu, Steve Ramirez, and Roger Reardon. Memory engram cells have come of age. *Neuron*, 87(5):918–931, 2015. 2
- [41] Ashish Vaswani, Noam Shazeer, Niki Parmar, Jakob Uszkoreit, Llion Jones, Aidan N Gomez, Łukasz Kaiser, and Illia Polosukhin. Attention is all you need. In I. Guyon, U. Von Luxburg, S. Bengio, H. Wallach, R. Fergus, S. Vishwanathan, and R. Garnett, editors, *Advances in Neural Information Processing Systems*, volume 30. Curran Associates, Inc., 2017. 1
- [42] Huanyu Wang, Wenhu Zhang, Shihao Su, Hui Wang, Zhenwei Miao, Xin Zhan, and Xi Li. Sp-net: Slowly progressing dynamic inference networks. In Shai Avidan, Gabriel Brostow, Moustapha Cissé, Giovanni Maria Farinella, and Tal Hassner, editors, *Computer Vision – ECCV 2022*, pages 223–240, Cham, 2022. Springer Nature Switzerland. 2
- [43] Ji Wang, Bokai Cao, Philip Yu, Lichao Sun, Weidong Bao, and Xiaomin Zhu. Deep learning towards mobile applications. In *2018 IEEE 38th International Conference on Distributed Computing Systems (ICDCS)*, pages 1385–1393, 2018. 2
- [44] Yisen Wang, Xingjun Ma, Zaiyi Chen, Yuan Luo, Jinfeng Yi, and James Bailey. Symmetric cross entropy for robust learning with noisy labels. In *2019 IEEE/CVF International Conference on Computer Vision (ICCV)*, pages 322–330, 2019. 2
- [45] Yingchun Wang, Jingyi Wang, Weizhan Zhang, Yufeng Zhan, Song Guo, Qinghua Zheng, and Xuanyu Wang. A survey on deploying mobile deep learning applications: A systemic and technical perspective. *Digital Communications and Networks*, 8(1):1–17, 2022. 2
- [46] Ross Wightman. Pytorch image models. <https://github.com/rwightman/pytorch-image-models>, 2019. 5
- [47] Jeremy M. Wolfe. Guided search 6.0: An updated model of visual search. *Psychonomic Bulletin & Review*, 28(4):1060–1092, Aug 2021. 1, 7
- [48] Sanghyun Woo, Shoubhik Debnath, Ronghang Hu, Xinlei Chen, Zhuang Liu, In So Kweon, and Saining Xie. Convnext v2: Co-designing and scaling convnets with masked autoencoders. In *2023 IEEE/CVF Conference on Computer Vision and Pattern Recognition (CVPR)*, pages 16133–16142, 2023. 8
- [49] Wenhan Xia, Hongxu Yin, Xiaoliang Dai, and Niraj K. Jha. Fully dynamic inference with deep neural networks. *IEEE Transactions on Emerging Topics in Computing*, 10(2):962–972, 2022. 3
- [50] Hong Xie, Yu Liu, Youzhi Zhu, Xinlu Ding, Yuhao Yang, and Ji-Song Guan. In vivo imaging of immediate early gene expression reveals layer-specific memory traces in the mammalian brain. *Proceedings of the National Academy of Sciences*, 111(7):2788–2793, 2014. 2, 3
- [51] Mengqi Xue, Jie Song, Li Sun, and Mingli Song. Tree-like branching network for multi-class classification. In Pandian Vasant, Ivan Zelinka, and Gerhard-Wilhelm Weber, editors, *Intelligent Computing & Optimization*, pages 175–184, Cham, 2022. Springer International Publishing. 2, 3

- [52] Jiahui Yu, Zirui Wang, Vijay Vasudevan, Legg Yeung, Mojtaba Seyedhosseini, and Yonghui Wu. Coca: Contrastive captioners are image-text foundation models, 2022. 2
- [53] Zizhao Zhang, Han Zhang, Long Zhao, Ting Chen, Serkan Ö. Arik, and Tomas Pfister. Nested hierarchical transformer: Towards accurate, data-efficient and interpretable visual understanding. In *AAAI Conference on Artificial Intelligence*, 2021. 2